

Magic gap ratio for optimally robust fermionic condensation and its implications for high- T_c superconductivity

N. Harrison and M. K. Chan

National High Magnetic Field Laboratory, Los Alamos National Laboratory, Los Alamos, NM 87545, USA

(Dated: May 12, 2022)

Bardeen-Schrieffer-Cooper (BCS) and Bose-Einstein condensation (BEC) occur at opposite limits of a continuum of pairing interaction strength between fermions. A crossover between these limits is readily observed in a cold atomic Fermi gas. Whether it occurs in other systems such as the high temperature superconducting cuprates has remained an open question. We uncover here unambiguous evidence for a BCS-BEC crossover in the cuprates by identifying a universal magic gap ratio $2\Delta/k_B T_c \approx 6.5$ (where Δ is the pairing gap and T_c is the transition temperature) at which paired fermion condensates become optimally robust. At this gap ratio, corresponding to the unitary point in a cold atomic Fermi gas, the condensate fraction N_0 and the height of the jump $\delta\gamma(T_c)$ in the coefficient γ of the fermionic specific heat at T_c are strongly peaked. In the cuprates, $\delta\gamma(T_c)$ is peaked at this gap ratio when Δ corresponds to the antinodal spectroscopic gap, thus reinforcing its interpretation as the pairing gap. We find the peak in $\delta\gamma(T_c)$ also to coincide with a normal state maximum in γ , which is indicative of a pairing fluctuation pseudogap above T_c .

A crossover in the pairing interactions between the weak coupling Bardeen-Schrieffer-Cooper (BCS) [1] and the strong coupling Bose-Einstein Condensation (BEC) [2, 3] limits was proposed in the high transition temperature T_c superconducting cuprates soon after their discovery [4–8]. On the BCS side, pairing takes place at the Fermi surface below T_c as in a conventional superconductor, whereas on the BEC side, fermions pair up to produce bosons whose subsequent condensation at T_c is determined by the phase stiffness of the superfluid. Whereas the cuprates provided the motivation for much of the early theoretical work on the BCS-BEC crossover, today it is in a cold atomic Fermi gas [9, 10] where this phenomenon is well established. The relative simplicity of a cold atomic Fermi gas, consisting of pairing interactions tuned via a Feshbach resonance in an otherwise weakly interacting Fermi gas, has made it the ideal paradigm for cementing [11–13] our theoretical understanding of condensation in the crossover region [8, 14]. Yet the question of whether such a crossover occurs in other paired fermion systems such as the cuprates has remained. The other proposed BCS-BEC crossover candidates include nuclear matter, quark-gluon plasmas, iron-based superconductors and twisted graphene [15–21].

While various experiments are suggestive of a non BCS pairing scenario in the cuprates [22–28], uncertainty has surrounded the question of whether T_c is a sufficiently large fraction of the Fermi temperature T_F for a BCS-BEC crossover to be viable [18]. For example, electronic band theory predicts a ratio $T_c/T_F \sim 10^{-2}$ that is clearly too small for a BCS-BEC crossover to occur [10]. However, thermodynamic measurements, including magnetic quantum oscillations, have revealed strongly renormalized quasiparticle effective masses [29]. It can be argued on the basis of such measurements that the ratio is close to that $T_c/T_F = 1/8$ required to be in the BCS-BEC crossover regime of a two-dimensional super-

conductor [18, 29]. Yet, given the increased effective mass renormalizations at low temperatures [55, 56] and various poorly understood phenomena such as the Fermi surface reconstruction [57, 58] and ‘Fermi arcs [29, 59],’ it is unclear whether the parabolic band approximation upon which T_F estimates are based [18] is valid in the cuprates.

Studies aiming to address the question of whether a BCS-BEC crossover occurs in the cuprates [15, 16, 62] have instead focused on the pseudogap [63], which is a partial gap in the fermionic density of states above T_c . In a cold atomic Fermi gas, a pseudogap is reported to develop in the BEC-BCS crossover region [64–67], and is unambiguously the result of normal state pairing correlations [15, 16, 62, 67–70]. In the cuprates, the pseudogap is maximal in the antinodal region of momentum-space where the d -wave pairing gap is maximal [63]. But while pairing has been proposed as the origin of the pseudogap in the cuprates [15, 62, 63, 71], antiferromagnetic correlations and unconventional broken symmetry phases have also been proposed to produce a pseudogap [72–77].

In this paper, we show that the key to establishing a universal thermodynamic signature of the BCS-BEC crossover, is the identification of a magic gap ratio [78, 79] $2\Delta/k_B T_c \approx 6.5$ at which paired fermion condensates become optimally robust [16]; throughout, we use Δ to refer to the magnitude of the pairing gap at low T [14, 66, 80]. At this gap ratio, corresponding to the unitary point in a cold atomic Fermi gas, experimental indicators of a robust condensate exhibit a sharp peak. These include the condensate fraction N_0 and the height of the jump $\delta\gamma(T_c)$ in the fermionic (or electronic) contribution $C = \gamma T$ to the specific heat at T_c (see schematic in Fig. 1a). In the cuprates, we find $\delta\gamma(T_c)$ to be peaked at the magic gap ratio when Δ corresponds to the antinodal gap [81]. Reinforcing its interpretation as the pairing gap [15, 62, 63, 71], we find (i) nearly identical asymmetric line shapes of $\delta\gamma(T_c)$ versus $2\Delta/k_B T_c$ in the cuprates

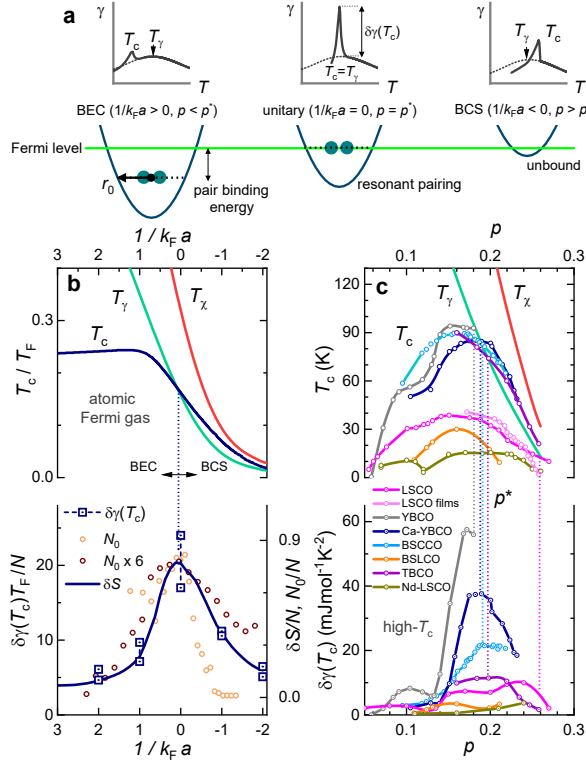


FIG. 1. **a**, Schematic $\gamma(T)$ with (solid lines) and without (dotted lines) a phase transition. Because of the transition, the normal state maximum is visible only when $T_\gamma > T_c$ (or $1/k_F a > 0$ or $p < p^*$). Also shown is a schematic of resonant pairing, occurring when the bound state energy coincides with the Fermi level [29], producing a sharp peak in $\delta\gamma(T_c)$. **b**, Unitary regime of a Fermi gas [8, 14]. Upper panel: T_c from Ref. [14] and $T_\gamma = 2\Delta/6.5k_B$ and $T_\chi = 2\Delta/3k_B$ (using Δ at the lowest T from Ref. [14]). Lower panel: $\delta\gamma(T_c)$ (lower and upper bound estimates extracted [29] from $S(T)$ in Fig. 5 of Ref. [14]), δS (from Fig. 6 of Ref. [14]; this closely follows $\delta\gamma(T_c)$, providing a guide to the eye), and N_0 (brown [13] and yellow [12] circles). **c**, Cuprates. Upper panel: $T_c(p)$ [56, 84–90, 119] and T_γ and T_χ from Fig. 2d. Lower panel: $\delta\gamma(T_c)$; Spline fits connect points. In (b) and (c), dotted lines indicate $p = p^*$ (for each cuprate family [90]) and $1/k_F a = 0$, at which $T_\gamma = T_c$, coinciding approximately with peaks in $\delta\gamma(T_c)$.

as for the unitary regime of a Fermi gas and (ii) coincidence of the peak in $\delta\gamma(T_c)$ with a normal state maximum in γ . The latter, along with an accompanying maximum in the spin susceptibility χ , can be understood as a signature of normal state pair amplitude fluctuations.

In the unitary regime of a Fermi gas, corresponding to $1 \gtrsim 1/k_F a \gtrsim -1$ in Figs. 1a and b, continuous tuning of the pairing interactions through the crossover occurs by way of the dimensionless parameter $1/k_F a$ [82], where a is the pair scattering length and k_F is the Fermi radius. The BCS side [1] corresponds to $k_F a < 0$, while the BEC side corresponds to $k_F a > 0$. The divergence in the elastic scattering cross section at $1/k_F a = 0$, which defines the location of the unitary point, causes the condensate to become optimally robust. This leads to peaks in $\delta\gamma(T_c)$ and

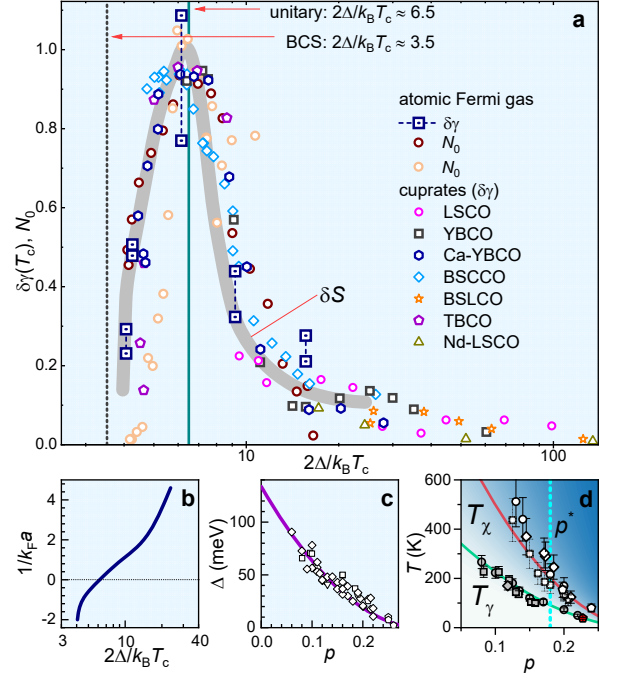


FIG. 2. **a**, $\delta\gamma(T_c)$, N_0 and δS (rescaled to unity from Figs. 1b and c) versus $2\Delta/k_B T_c$. **b**, $1/k_F a$ versus $2\Delta/k_B T_c$ [14]. **c**, Spectroscopic and thermal antinodal gap measurements [71, 101, 102]. **d**, Maxima in γ (grey symbols) and χ (white symbols) from the raw data [29]. T_γ (green line) is a polynomial fit to the grey symbols [100], from which we obtain $\Delta = 6.5k_B T_\gamma/2$ (i.e. the purple line in (d)) and $T_\chi = 2\Delta/3k_B$ (red line). Symbol shapes identify the cuprate family in (a), (c) and (d). The down triangle in (c) refers to HBCO [90].

in the entropy change δS accompanying condensation at T_c [14, 29] (see Fig. 1b). An optimally robust condensate is confirmed experimentally by the observation of a peak in N_0 as a function of $1/k_F a$ (see Fig. 1b) [12, 13, 29] and a maximally large $\delta\gamma(T_c)$ [11, 83], which also occurs at the value of T_c predicted by theory [14].

Turning to the cuprates in Fig. 1, the measured $\delta\gamma(T_c)$ changes by as much as a factor of ~ 30 in YBCO [56, 84–90]. This change is far larger than the variations in $\delta\gamma(T_c)$ that are ordinarily explained by Eliashberg theory in regular BCS systems [29, 78, 79], or have been predicted in various strongly coupled pairing models of the cuprates [94–96]. The $\delta\gamma(T_c)$ curves do, however, exhibit maxima as a function of p resembling the behavior as a function of $1/k_F a$ in the unitary regime of a Fermi gas in Fig. 1b.

The similar behavior of the cuprates to the unitary regime of a Fermi gas becomes clear once the data from Figs. 1b and c are replotted on the same $2\Delta/k_B T_c$ axis in Fig. 2a. While $2\Delta/k_B T_c$ is not a tuning parameter, it has the advantage in that it can be determined in both systems. In a cold atomic Fermi gas, there exists a direct correspondence between $1/k_F a$ and $2\Delta/k_B T_c$ [14, 97] (see Fig. 2b). Studies of the unitary regime differ on the precise values of Δ and T_c at the unitary point [4, 7–

10, 15, 16, 62, 98]. However, they are found to be consistent with respect to the ratio $2\Delta/k_B T_c = 6.5 \pm 0.2$ [29] (see for example Fig. 9 of Ref. [97] and Table 1 of Ref. [16]), indicating this magic gap ratio to be a robust property of such a point.

Various non cuprate superconductors, including classic BCS [78] and iron-based systems [79], while spanning comparatively limited ranges in $2\Delta/k_B T_c$, are found to exhibit trends in $\delta\gamma(T_c)/\bar{\gamma}$ versus $2\Delta/k_B T_c$ consistent with Fig. 2a [29]. In these systems, dividing by an assumed constant Sommerfeld coefficient $\bar{\gamma}$ enables universal trends in $\delta\gamma(T_c)$ to be established [29] for materials with different electronic structures. The iron-based superconductors with the highest $\delta\gamma(T_c)/\bar{\gamma}$ values are found to have gap ratios consistent with the magic value. Of these, iron selenide has also recently been reported to exhibit a BCS-BEC crossover [20, 21] — albeit without accompanying measurements of $\delta\gamma(T_c)$. A similar gap ratio at unitarity is further reported in gated layered superconductors [99].

The asymmetric line shape in Fig. 2a can be understood to result from the fact that the gap ratio has a hard cutoff on the left-hand side at a value similar to that ≈ 3.5 of an ideal BCS superconductor [1], while there is no cutoff on the BEC side [4, 7–10, 15, 16, 62]. On the BCS side, $\delta\gamma(T_c)$ increases with $2\Delta/k_B T_c$ similarly to that in Eliashberg theory [29, 78], while on the BEC side, T_c and consequently $\delta\gamma(T_c)$ are limited by the phase stiffness of the condensate [23]. We find precisely this line shape in the cuprates when Δ (purple line in Fig. 2c) [29, 100] corresponds to the antinodal gap dominating spectroscopic and thermodynamic measurements (symbols in Fig. 2c) [71, 101, 102]. The same asymmetric behavior is displayed for multiple cuprate families [56, 84–89]. On averaging the values of $2\Delta/k_B T_c$ in Fig. 2a at which $\delta\gamma(T_c)$ is peaked (near $p \approx 0.2$ in Fig. 1c) for the higher T_c cuprates (YBCO, Ca-YBCO, BSCCO and TBCO [90]), we obtain $2\Delta/k_B T_c = 6.4 \pm 0.3$, which is the same within experimental uncertainty as for a unitary Fermi gas. Validity of the universal magic gap ratio is therefore strongly suggested in the cuprates.

The association of Δ with the antinodal gap in the cuprates is reinforced by thermodynamic evidence for pairing correlations in the normal state. In the cuprates, normal state pair amplitude fluctuations associated with the pseudogap have been proposed to account for maxima in γ and χ as a function of T [94–96, 103]. Pair amplitude fluctuations in the unitary and BEC regimes of a Fermi gas also produce normal state maxima in γ (or $C = \gamma T$) [29, 104] and χ [69, 70, 105, 106]. Figure 3 shows that on plotting γ [87, 107] and χ [87, 91, 92, 108–113] versus $2\Delta/k_B T$, maxima in γ and χ emerge as ubiquitous properties of the normal state (in the cuprates, the shape of χ versus T is provided by magnetic susceptibility χ_m and nuclear magnetic resonance Knight shift K measurements [114]). The model γ and χ curves (black

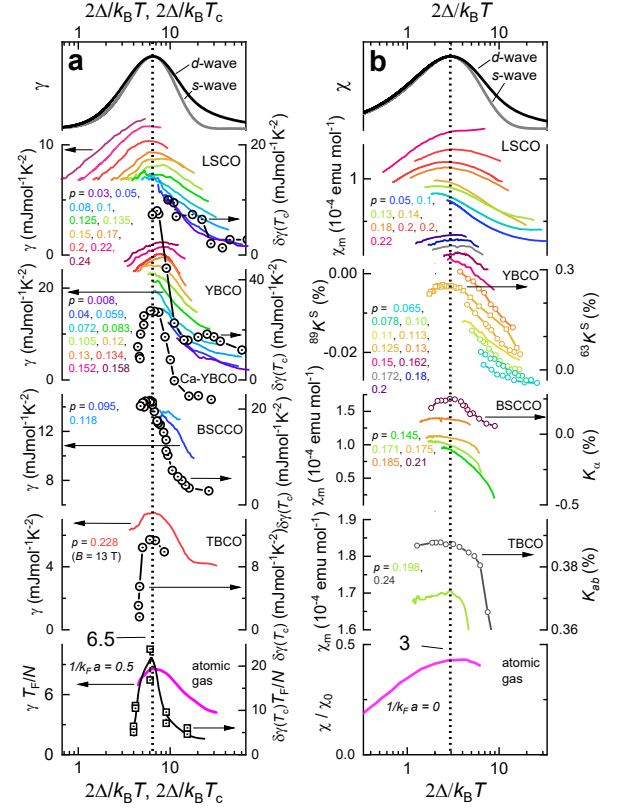


FIG. 3. **a**, Left-hand axes: γ for $T > T_c$ [29, 30, 62, 84, 87, 107] (colored lines; including 2% Zn substitution for the highest 2 YBCO dopings [107]) versus $2\Delta/k_B T$; p and $1/k_F a$ values are indicated throughout. Right-hand axes: $\delta\gamma(T_c)$ at T_c versus $2\Delta/k_B T_c$ for the cuprates [56, 84–88] (center-dot circles; shifted by $\pm 10 \text{ mJmol}^{-1} \text{K}^{-2}$ for YBCO and Ca-YBCO) and a Fermi gas from Fig. 1 (center-dot squares). **b**, χ_m [87, 92, 109, 110], K [91, 108, 111–113] and χ [105] versus $2\Delta/k_B T$ [114]. Included are γ and χ for model d - (black) and s -wave (grey) gaps of magnitude Δ [29]. Some YBCO K curves are shifted vertically for clarity and spline fits connect coarsely spaced points. Dotted lines indicate $2\Delta/k_B T_c = 6.5$ and $2\Delta/k_B T = 3$.

and grey in Fig. 3) produced by an excitation gap of width Δ [29, 81] exhibit maxima at $T_\gamma \approx 2\Delta/6.5k_B$ and $T_\chi \approx 2\Delta/3k_B$. A pairing pseudogap [115] is strongly suggested in the cuprates by the consistency of the observed maxima in Fig. 3 with T_γ and T_χ . In fact, we find overall consistency between each of the $\Delta(p)$, $T_\gamma(p)$ and $T_\chi(p)$ curves and the experimental data points for the antinodal gap and maxima in γ and χ [29] in Figs. 2c and d. Thermodynamic and spectroscopic measurements can therefore both be understood in terms of a $\Delta(p)$ that is approximately the same for all cuprate families, regardless of their optimal T_c .

A direct association of the normal state maxima with pairing amplitude fluctuations is strongly suggested by the alignment of the maxima in γ with the peaks in $\delta\gamma(T_c)$ when γ and $\delta\gamma(T_c)$ are respectively plotted versus $2\Delta/k_B T$ and $2\Delta/k_B T_c$ in Fig. 3a. Since $2\Delta/k_B T$ and

$2\Delta/k_B T_c$ are both scaled by Δ , the alignments of γ and $\delta\gamma(T_c)$ are independent of any experimental uncertainties in the functional form of $\Delta(p)$ [100]. We find the alignments to originate from $\delta\gamma(T_c)$ being peaked close to the points of intersection of T_c with T_γ (see Figs. 1b and c), corresponding to $1/k_F a = 0$ (i.e. the unitary point) in a unitary Fermi gas and a characteristic doping $p = p^*$ in the cuprates.

In the unitary regime of a Fermi gas, $\delta\gamma(T_c)$ exhibiting a strong peak at $T_c = T_\gamma$ can be understood as a consequence of the heavily broadened pseudogap transitioning into a regular pairing gap [115] as long range phase coherence is established below T_c [116, 117]. The entropy change contributing to $\delta\gamma(T_c)$ is naturally largest when T_c coincides with the maximum in γ resulting from excitations across Δ . This is therefore suggested also to occur in the cuprates at $T_c = T_\gamma$ [29]. $\delta\gamma(T_c)$ exhibiting a strong peak at $T_c = T_\gamma$ can also be understood as a consequence of the normal state entropy S_n at T_c (in addition to δS) exhibiting a maximum (as a function of $1/k_F a$) close to this point, owing to this region of the normal state consisting of a maximally disordered mixture of a bosonic and fermionic degrees of freedom [14, 104]. At $T > T_c$, a peak in $S_n(1/k_F a)$ is also seen to extend vertically in T at the unitary point [9, 14], with the loss of fermion degrees of freedom at $1/k_F a > 0$ leading to a sharp drop S_n on the BEC side of the phase diagram. An examination of S_n in several cuprates [118] reveals that this too exhibits a sharp peak that extends vertically in T near p^* , accompanied by a drop in S_n at $p < p^*$.

One consequence of $\delta\gamma(T_c)$ being peaked close to the point of intersection of T_γ and T_c is that p^* is distinct from the hole doping $p \approx 0.16$ at which T_c is optimal. In fact, p^* moves towards the upper end of the superconducting dome as the optimal T_c is reduced, and appears to be accompanied by a strong suppression of the overall peak height of $\delta\gamma(T_c)$. In LSCO, for example, an extrapolation of T_γ in Fig. 1c suggests that $p^* \approx 0.26 \pm 0.03$, which is consistent with the higher value of $p = 0.23 \pm 0.1$ (compared e.g. to YBCO) at which $\delta\gamma(T_c)$ is peaked [29] and the higher value of $p = 0.24 \pm 0.01$ (compared to Ca-YBCO) at which S_n is peaked [118]. In LSCO films, by contrast, T_c lies significantly below T_γ in Fig. 1c, suggesting that they do not exhibit a crossover into the BCS regime, as has also been suggested on the basis of the superfluid density measurements [29, 119]. The tiny p -dependent $\delta\gamma(T_c)$ in Nd-LSCO, meanwhile, suggests that its peak value occurs at higher dopings than have been accessed experimentally [56, 120].

Given the prior reports of quantum criticality in the cuprates at similar hole dopings to p^* [121–123], one intriguing possibility is that the BCS-BEC crossover and quantum criticality share a common origin. Indeed, some of the reported phenomenology of quantum criticality in the cuprates bears similarities to that of the unitary regime of a Fermi gas [124]. This includes Plankian dis-

sipation and scale invariance [121–126], and a minimum in the pair coherence length [17, 127, 128] inferred from the maximum in the superconducting upper critical magnetic field [29, 55, 93, 129]. It should be noted, however, that thermodynamic evidence for quantum criticality in the form of a sharply increasing γ or an upturn in the effective mass, has thus far only been reported at low temperatures ($T \ll 10$ K) [55, 56], and has yet to be accompanied by evidence for a divergence in the correlation length of a broken symmetry phase [29].

Supported by the Department of Energy (DoE) BES project ‘Science of 100 tesla.’ The National High Magnetic Field Laboratory is funded by NSF Cooperative Agreements DMR-1157490 and 1164477, the State of Florida and DoE. We thank John Cooper, Mohit Randeria, Patrick Lee, Arkady Shekter, John Singleton, Greg Boebinger and Giancarlo Strinati for helpful discussions.

-
- [1] Bardeen, J., Cooper, L. N., Schrieffer, J. R. Theory of superconductivity. *Phys. Rev.* **108**, 1175-1204 (1957).
 - [2] Jochim, S., Bartenstein, M., Altmeyer, A., Hendl, G., Riedl, S., Chin, C., Denschlag, J.H., Grimm, R., Bose-Einstein condensation of molecules, *Science* **302**, 2101-2103 (2003).
 - [3] Zwierlein, M.W., Stan, C.A., Schunck, C.H., Raupach, S.M.F., Gupta, S., Hadzibabic, Z., Ketterle, W., Observation of Bose-Einstein condensation of molecules, *Phys. Rev. Lett.* **91**, 250401 (2003).
 - [4] Randeria, M., Duan, J.-M., Shieh, L.-Y., Bound states, Cooper pairing, and Bose condensation in two dimensions, *Phys. Rev. Lett.* **62**, 981-984 (1989).
 - [5] Friedberg, R., Lee, T. D., Gap energy and long-range order in the boson-fermion model of superconductivity. *Phys. Rev. B* **40**, 6745-6762 (1989).
 - [6] Micnas, R., Ranninger, J., Robaszkiewicz, S., Superconductivity in narrow-band systems with local nonretarded attractive interactions. *Rev. Mod. Phys.* **62**, 113-171 (1990).
 - [7] Drechsler, M., Zwerger, W., Crossover from BCS-superconductivity to Bose-condensation. *Ann. Physik* **1**, 15-23 (1992).
 - [8] Sá de Melo, C. A. R., Randeria, M., Engelbrecht, J. R., Crossover from BCS to Bose superconductivity: transition temperature and time-dependent Ginzburg-Landau theory. *Phys. Rev. Lett.* **71**, 3202-3205 (1993).
 - [9] Bloch, I., Dalibard, J., Zwerger, W., Many-body physics with ultracold gases. *Rev. Mod. Phys.* **80**, 885-964 (2008).
 - [10] Giorgini, S., Pitaevskii, L. P., Stringari, S., Theory of ultracold atomic Fermi gases. *Rev. Mod. Phys.* **80**, 1215-1274 (2008).
 - [11] Ku, M. J. H., Sommer, A. T., Cheuk, L. W., Zwierlein, M. W., Revealing the superfluid Lambda transition in the universal thermodynamics of a unitary Fermi gas. *Science* **335**, 563-567 (2012).
 - [12] Regal, C. A., Greiner, M., Jin, D. S., Observation of resonance condensation of fermionic atom pairs. *Phys. Rev. Lett.* **92**, 040403 (2004).

- [13] Zwierlein, M. W., Stan, C. A., Schunck, C. H., Raupach, S. M. F., Kerman, A. J., Ketterle, W., Condensation of pairs of Fermionic atoms near a Feshbach resonance. *Phys. Rev. Lett.* **92**, 120403 (2004).
- [14] Haussmann, R., Rantner, W., Cerrito, S., Zwerger, W., Thermodynamics of the BCS-BEC crossover. *Phys. Rev. A* **75**, 023610 (2007).
- [15] Chen, Q., Stajic, J., Tan, S., Levin, K. BCS-BEC crossover: From high temperature superconductors to ultracold superfluids. *Phys. Reports* **412**, 1-88 (2005).
- [16] Randeria, M., Taylor, E., Crossover from Bardeen-Cooper-Schrieffer to Bose-Einstein condensation and the unitary Fermi gas. *Annu. Rev. Condens. Matter Phys.* **5**, 209-232 (2014).
- [17] Strinati, G. C., Pieri, P. P., Röpke, G., Schuck, P., Urban, M. The BCS-BEC crossover: From ultra-cold Fermi gases to nuclear systems. *Phys. Rep.* **738**, 1-76 (2018).
- [18] Hazra, T., Verma, N., Randeria, M., Bounds on the superconducting transition temperature: applications to twisted bilayer graphene and cold atoms. *Physical Review X* **9**, 031049 (2019).
- [19] Park, J. M., Cao, Y., Watanabe, K., Taniguchi, T., Jarillo-Herrero, P., Tunable strongly coupled superconductivity in magic-angle twisted trilayer graphene. *Nature* **590**, 249-255 (2021).
- [20] Kasahara, S., Watashige, T., Hanaguri, T., Kohsaka, Y., Yamashita, T., Shimoyama, Y., Mizukami, Y., Endo, R., Ikeda, H., Aoyama, K., Terashima, T., Uji, S., Wolf, T., von Lohneysen, H., Shibauchi, T., Matsuda, Y. Field-induced superconducting phase of FeSe in the BCS-BEC cross-over. *Proc. Nat. Acad. Sci. USA* **111**, 116309-16313 (2014).
- [21] Rinott, S., Chashka, K. B., Ribak, A., Rienks, E. D. L., Taleb-Ibrahimi, A., Le Fevre, P., Bertran, F., Randeria, M., Kanigel, A., Tuning across the BCS-BEC crossover in the multiband superconductor $\text{Fe}_{1+y}\text{Se}_x\text{Te}_{1-x}$: An angle-resolved photoemission study. *Sci. Adv.* **3**, 1602372 (2017).
- [22] Uemura, Y. J., Luke, G. M., Sternlieb, Brewer, J. H., Carolan, J. F., Hardy, W. N., Kadono, R., Kempton, J. R., Kiefl, R. F., Kreitzman, S. R., Mulhern, P., Rise-man, T. M., Williams, D. L., Yang, B. X., Uchida, S., Takagi, H., Gopalakrishnan, J., Sleight, A. W., Suba-manian, M. A., Chien, C. L., Cieolak, M. Z., Xiao, G., Lee, V. Y., Statt, N. W., Stronach, C. E., Kossler, W. J., Yu, X. H., Universal correlations between T_c and n_s/m^* (carrier density over effective mass) in high- T_c cuprate superconductors. *Phys. Rev. Lett.* **62**, 2317-2320 (1989).
- [23] Emery, V.J., Kivelson, S.A., Importance of phase fluctuations in superconductors with small superfluid density. *Nature* **374**, 434-437 (1995).
- [24] Li, L., Wang, Y., Komiyama, S., Ono, S., Ando, Y., Gu, G.D., Ong, N.P. Diamagnetism and Cooper pairing above T_c in cuprates. *Phys. Rev. B* **81**, 054510 (2010).
- [25] Dubroka, A., Rössle, M., Kim, K.W., Malik, V.K., Munzar, D., Basov, D.N., Scafars, A.A., Moon, S.J., Lin, C.T., Haug, D., Hinkov, V., Keimer, B., Wolf, Th., Storey, J.G., Tallon, J.L., Bernhard, C., Evidence of a precursor superconducting phase at temperatures as high as 180 K in $R\text{Ba}_2\text{Cu}_3\text{O}_{7-\delta}$ ($R = \text{Y, Gd, Eu}$) superconducting crystals from infrared spectroscopy. *Phys. Rev. Lett.* **106**, 047006 (2011).
- [26] Hu, W., Kaiser, S., Nicoletti, D., Hunt, C.R., Gierz, I., Homann, M.C., Le Tacon, M., Loew, T., Keimer, B., Cavalleri, A., Optically enhanced coherent transport in $\text{YBa}_2\text{Cu}_3\text{O}_{6.5}$ by ultrafast redistribution of interlayer coupling. *Nature Materials* **13**, 705-711 (2014).
- [27] Kaiser, S., Hunt, C.R., Nicoletti, D., Hu, W., Gierz, I., Liu, H.Y., Le Tacon, M., Loew, T., Haug, D., Keimer, B., Cavalleri, A., Optically induced coherent transport far above T_c in underdoped $\text{YBa}_2\text{Cu}_3\text{O}_{6+\delta}$. *Phys. Rev. B* **89**, 184516 (2014).
- [28] Zhou, P., Chen, L., Liu, Y., Sochnikov, I., Bollinger, A. T., Han, M.-G., Zhu, Y., He, X., Božović, I., Natelson, D., Electron pairing in the pseudogap state revealed by shot noise in copper oxide junctions. *Nature* **572**, 493-496 (2019).
- [29] See Supplementary Information, which discusses data pertaining to $\delta\gamma(T_c)$ in conventional BCS and Fe- and Ni based superconductors; information about cuprate hole dopings p used in constructing graphs; raw γ and χ data including the locations of T_γ and T_χ ; Knight shift data on BLSCO; a discussion pertaining to prior modeling of $\delta\gamma(T_c)$ versus p by Chen *et al.*; details concerning cold atomic gas data used; estimates of the gap ratio at the unitary point of a cold atomic gas; a discussion of the thermodynamics of maxima in γ and χ ; coherence length estimates in various cuprates based on H_{c2} ; estimates of the Fermi energy in the cuprates; a discussion of the higher values of p^* in cuprates with lower T_c 's; the origin of 'Fermi arcs'; the T -dependence of the antinodal gap; lifetime effects on N_0 ; problems with a smaller gap option for Δ in the cuprates; a hidden maximum in the heat capacity of a cold atomic Fermi gas; reports of peaks in $\delta\gamma(T_c)$, γ and m^* associated with quantum criticality, and includes Refs. [30–54].
- [30] Radcliffe, J.W., Loram, J.W., Wade, J.M., Wltschek, G., Tallon, J.W., Electronic specific heat of overdoped $\text{Ti}_2\text{Ba}_2\text{CuO}_{6+\delta}$ in a magnetic field. *J. Low. Temp. Phys.* **105**, 903-908 (1996).
- [31] Takagi, H., Ido, T., Ishibashi, S., Uota, M., Uchida, S., Tokura, Y., Superconductor-to-nonsuperconductor transition in $(\text{La}_{1-x}\text{Sr}_x)_2\text{CuO}_4$ as investigated by transport and magnetic measurements. *Phys. Rev. B* **40**, 2254-2261 (1989).
- [32] Liang, R., Bonn, D. A., Hardy, W. N. Evaluation of CuO_2 plane hole doping in $\text{YBa}_2\text{Cu}_3\text{O}_{6+x}$ single crystals. *Phys. Rev. B* **73**, 180505 (2006).
- [33] Zhou, J.-S., Goodenough, J.B., Dabrowski, B., Rogacki, K., Transport properties of a $\text{YBa}_2\text{Cu}_4\text{O}_8$ crystal under high pressure. *Phys. Rev. Lett.* **77**, 4253-4256 (1996).
- [34] Tallon, J.L., Bernhard, C., Shaked, H., Hitterman, R.L., Jorgensen, J.D., Generic superconducting phase-behavior in high- T_c variation with hole concentration in $\text{YBa}_2\text{Cu}_3\text{O}_{7-\delta}$. *Phys. Rev. B* **51**, 12911-12914 (1995).
- [35] Meingast, C., Inaba, A., Heid, R., Pankoke, V., Bohnen, K.-P., Reichardt, W., Wolf, T., Specific-heat of $\text{YBa}_2\text{Cu}_3\text{O}_x$ up to 400 K: high-resolution adiabatic measurements and *Ab-initio* LDA phonon calculations. *J. Phys. Soc. Japan* **78**, 074706 (2009).
- [36] Kawasaki, S., Lin, C., Kuhns, P.L., Reyes, A.P., Zheng, G.-Q., Carrier-concentration dependence of the pseudogap ground state of superconducting $\text{Bi}_2\text{Sr}_{2-x}\text{La}_x\text{CuO}_{6+\delta}$ revealed by $^{63,65}\text{Cu}$ -nuclear magnetic resonance in very high magnetic fields. *Phys. Rev. Lett.* **105**, 137002 (2010).
- [37] Kittel, C., Introduction to Solid State Physics, eighth

- ed. (Wiley, New York, 2004).
- [38] Nolthing, W., Ramakanth, A., Quantum Theory of Magnetism (Springer, New York, 2009).
 - [39] Suzuki M., Hikita, M., Resistive transition, magnetoresistance, and anisotropy in $\text{La}_{2-x}\text{Sr}_x\text{CuO}_4$ single-crystal thin films. *Phys. Rev. B* **44**, 249-261 (1991).
 - [40] Rourke, P. M. C., Bangura, A. F., Benseman, T. M., Matusiak, M., Cooper, J. R., Carrington, A., Hussey, N. E., A detailed de Haas-van Alphen effect study of the overdoped cuprate $\text{Tl}_2\text{Ba}_2\text{CuO}_{6+\delta}$, *New J. Phys.* **12**, 105009 (2010).
 - [41] LeBoeuf, D., Doiron-Leyraud, N., Levallois, J., Daou, R., Bonnemaïson, J. B., Hussey, N. E., Balicas, L., Ramshaw, B. J., Liang, R. X., Bonn, D. A., Hardy, W. N., Adachi, S., Proust, C., Taillefer, L. Electron pockets in the Fermi surface of hole-doped high- T_c superconductors. *Nature* **450**, 533-536 (2007).
 - [42] Rullier-Albenque, F., Alloul, H., Balakirev, F., Proust, C., Disorder, metal-insulator crossover and phase diagram in high- T_c cuprates. *EPL* **81**, 37008 (2008).
 - [43] Fukuzumi, Y., Mizuhashi, K., Takenaka, K., Uchida, S., Universal superconductor-insulator transition and T_c depression in Zn-substituted high- T_c cuprates in the underdoped regime. *Phys. Rev. Lett.* **76**, 684-687 (1996).
 - [44] Nachumi, B., Keren, A., Kojima, K., Larkin, M., Luke, G. M., Merrin, J., Tchernyshöf, O., Uemura, Y. J., Ichikawa, N., Goto, M., Uchida, S., Muon spin relaxation studies of Zn-substitution effects in high- T_c cuprate superconductors. *Phys. Rev. Lett.* **77**, 5421-5424 (1996).
 - [45] Carrington, A., Mackenzie, A. P., Sinclair, D. C., Cooper, J. R., Field dependence of the resistive transition in $\text{Tl}_2\text{Ba}_2\text{CuO}_{6+\delta}$. *Phys. Rev. B* **49**, 13243-13246 (1994).
 - [46] Chubukov, A.V., Norman, M.R., Millis, A.J., Abrahams, E., Gapless pairing and the Fermi arc in the cuprates. *Phys. Rev. B* **76**, 180501 (2007).
 - [47] de Mello, E.V.L., Disordered-based theory of pseudogap, superconducting gap, and Fermi arc of cuprates. *Euro. Phys. Lett.* **99**, 37003 (2012).
 - [48] Fradkin, E., Kivelson, S.A., Tranquada, J.M., Colloquium: Theory of intertwined orders in high temperature superconductors. *Rev. Mod. Phys.* **87**, 457-482 (2015).
 - [49] Agterberg, D.F., Davis, J.C.S., Edkins, S.D., Fradkin, E., Van Harlingen, D.J., Kivelson, S.A., Lee, P.A., Radzihovsky, L., The physics of pair-density waves: cuprate superconductors and beyond. *Annu. Rev. Condens. Matter Phys.* **11**, 231-270 (2020).
 - [50] Ding, H., Campuzano, J.C., Takahashi, T., Randeria, M., Norman, M.R., Mochikull, T., Kadowaki, K., Giapintzaki, J., Spectroscopic evidence for a pseudogap in the normal state of underdoped high- T_c superconductors. *Nature* **382**, 51-54 (1996).
 - [51] Renner, Ch., Revaz, B., Genoud, J.-Y., Kadowaki, K., Fischer, Ø., Pseudogap precursor of the superconducting gap in under- and overdoped $\text{Bi}_2\text{Sr}_2\text{CaCu}_2\text{O}_{8+\delta}$. *Phys. Rev. Lett.* **80**, 149-152 (1998).
 - [52] Mishra, V., Chatterjee, U., Campuzano, J. C., Norman, M. R., Effect of the pseudogap on the transition temperature in the cuprates and implications for its origin. *Nature Phys.* **10**, 357-360 (2014).
 - [53] Park, T., Graf, M. J., Boulaevskii, L., Sarrao, J. L., Thompson, J. D. Electronic duality in strongly correlated matter. *Proc. Nat. Acad. Sci. USA* **105**, 6825-6828 (2008).
 - [54] LeBlanc, J.P.F., Nicol, E.J., Carbotte, J.P., Specific heat of underdoped cuprates: Resonating valence bond description versus Fermi arcs. *Phys. Rev. B* **80**, 060505 (2009).
 - [55] Ramshaw, B. J., Sebastian, S. E., McDonald, R. D., Day, J., Tan, B. S., Zhu, Z., Betts, J.B., Liang, R.-X., Bonn, D.A., Hardy, W.N., Harrison, N., Quasiparticle mass enhancement approaching optimal doping in a high- T_c superconductor. *Science* **348**, 317-320 (2015).
 - [56] Michon, B., Girod, C., Badoux, S., Kačmarčík, J., Ma, Q., Dragomir, M., Dabkowska, H. A., Gaulin, B.D., Zhou, J.-S., Pyon, S., Takayama, T., Takagi, H., Verret, S., Doiron-Leyraud, N., Marcenat, C., Taillefer, L., Klein, T., Thermodynamic signatures of quantum criticality in cuprate superconductors. *Nature* **567**, 218-222 (2019).
 - [57] Sebastian, S.E., Harrison, N., Lonzarich, G.G. Towards resolution of the Fermi surface in underdoped high- T_c superconductors. *Rep. Prog. Phys.* **75**, 102501 (2012).
 - [58] The prevailing view [59] is that the Fermi surface reconstruction producing the pockets, for instance by a charge density wave [60, 61], cannot by itself account for the pseudogap.
 - [59] Keimer, B., Kivelson, S. A., Norman, M. R., Uchida, S., Zaanen, J. From quantum matter to high-temperature superconductivity in copper oxides. *Nature* **518**, 179-186 (2015).
 - [60] Hücker, Christensen, N.B., Holmes, A.T., Blackburn, E., Forgan, E.M., Liang, R., Bonn, D.A., Hardy, W.N., Gutowski, O., Zimmermann, M.v., Hayden, S.M., Chang, J., Competing charge, spin, and superconducting orders in underdoped $\text{YBa}_2\text{Cu}_3\text{O}_y$. *Phys. Rev. B* **90**, 054514 (2014).
 - [61] Blanco-Canosa, S., Frano, A., Schierle, E., Porras, J., Loew, T., Minola, M., Bluschke, M., Weschke, E., Keimer, B., Le Tacon, M., Resonant x-ray scattering study of charge-density wave correlations in $\text{YBa}_2\text{Cu}_3\text{O}_{6+x}$. *Phys. Rev. B* **90**, 054513 (2014).
 - [62] Chen, Q. and Wang, J., Pseudogap phenomena in ultracold atomic Fermi gases. *Front. Phys.* **9** 539-570 (2014).
 - [63] Timusk, T., Statt, B. The pseudogap in high-temperature superconductors: an experimental survey. *Rep. Prog. Phys.* **62**, 61-122 (1999).
 - [64] Gaebler, J. P., Stewart, J. T., Drake, T. E., Jin, D. S., Perali, A., Pieri, P., Strinati, G. C., Observation of pseudogap behaviour in a strongly interacting Fermi gas. *Nat. Phys.* **6**, 569-573 (2010).
 - [65] Magierski, P., Wlazłowski, G., Bulgac, A., Onset of a pseudogap regime in ultracold Fermi gases. *Phys. Rev. Lett.* **107**, 145304 (2011).
 - [66] Chin, C., Bartenstein, M., Altmeyer, A., Riedl, S., Jochim, S., Hecker Denschlag, J., Grimm, R., Observation of the pairing gap in a strongly interacting Fermi gas. *Science* **305**, 1128-1130 (2004).
 - [67] Perali, A., Palestini, F., Pieri, P., Strinati, G. C., Stewart, J. T., Gaebler, J. P., Drake, T. E., Jin, D. S., Evolution of the normal state of a strongly interacting Fermi gas from a pseudogap phase to a molecular Bose gas. *Phys. Rev. Lett.* **106**, 060402 (2011).
 - [68] Tsuchiya, S., Watanabe, R., Ohashi, Y., Single-particle properties and pseudogap effects in the BCS-BEC crossover regime of an ultracold Fermi gas above T_c .

- Phys. Rev. A* **80**, 033613 (2009).
- [69] Jensen, S., Gilbreth, C. N., Alhassid, Y. Pairing correlations across the superfluid phase transition in the unitary Fermi gas. *Phys. Rev. Lett.* **124**, 090604 (2020).
- [70] Richie-Halford, A., Drut, J. E., Bugac, A., Emergence of a pseudogap in the BCS-BEC crossover. *Phys. Rev. Lett.* **125** 060403 (2020).
- [71] Hufner, S., Hossain, M.A., Damascelli, A., Sawatsky, G.A., Two gaps make a high-temperature superconductor? *Rep. Prog. Phys.* **71**, 062501 (2008).
- [72] Chakravarty, S., Laughlin, R.B., Morr, D.K., Nayak, C., Hidden order in the cuprates. *Phys. Rev. B* **63**, 094503 (2001).
- [73] Lee, P. A., Nagaosa, N., Wen, X.-G. Doping a Mott insulator: Physics of high-temperature superconductivity. *Rev. Mod. Phys.* **78**, 17-85 (2006).
- [74] Varma, C.M., Theory of the pseudogap state of the cuprates. *Phys. Rev. B* **73**, 155113 (2006).
- [75] Rice, T.M., Yang, K.-Y., Zhang, F.C., A phenomenological theory of the anomalous pseudogap phase in underdoped cuprates. *Rep. Prog. Phys.* **75**, 016502 (2012).
- [76] Nie, L., Tarjus, G., Kivelson, S.A., Quenched disorder and vestigial nematicity in the pseudogap regime of the cuprates. *Proc. Nat. Acad. Sci. USA* **111**, 7980-7985 (2014).
- [77] Schmalian, J., Pines, D., Stojković, Microscopic theory of weak pseudogap behavior in the underdoped cuprate superconductors: General theory and quasiparticle properties. *Phys. Rev. B* **60**, 667-686 (1999).
- [78] Carbotte, J. P., Properties of boson-exchange superconductors. *Rev. Mod. Phys.* **62**, 1027-1157 (1990).
- [79] Inosov, D., S., Park, J. T., Charnukha, A., Yuan, L., Boris, A. V., Keimer, B., Hinkov, V., Crossover from weak to strong pairing in unconventional superconductors. *Phys. Rev. B* **83**, 214520 (2011).
- [80] Schirotzek, A., Shin, Y., Schunck, C. H., Ketterle, W., Determination of the superfluid gap in atomic Fermi gases by quasiparticle spectroscopy. *Phys. Rev. Lett.* **101**, 140403 (2008).
- [81] Since Fig. 2c includes spectroscopic data taken at low temperatures, we assume this to provide an estimate of Δ [29].
- [82] Leggett, A. J. in *Modern Trends in the Theory of Condensed Matter* (eds Pekalski, A. & Przysław, J.) 13-27 (Proc. XVIth Karpacz Winter School of Theoretical Physics, Springer, Berlin, 1980).
- [83] Zwerger, W. in *Proceedings of the International School of Physics "Enrico Fermi" — Course 191 "Quantum matter at ultralow temperatures"* (Inguscio, M., Ketterle, W., Roati, Q. eds.) 63-142 (IOS Press, Amsterdam; SIF Bologna, 2016).
- [84] Loram, J. W., Mirza, K. A., Cooper, J. R., Liang, W. Y. Electronic specific heat of $\text{YBa}_2\text{Cu}_3\text{O}_{6+x}$ from 1.8 to 300 K. *Phys. Rev. Lett.* **71**, 1740-1743 (1993).
- [85] Wade, J. M., Loram, J. W., Mirza, K. A., Cooper, J. R., Tallon, J. R., Electronic specific heat of $\text{Ti}_2\text{Ba}_2\text{CuO}_{6+\delta}$ from 2 K to 300 K for $0 \leq \delta \leq 0.1$. *J. Superconductivity* **7**, 261-264 (1994).
- [86] Loram, J. W., Mirza, K. A., Cooper, J. R., Tallon, J. L. Specific heat evidence of the normal state pseudogap. *J. Phys. Chem. Solids* **59**, 2091-2094 (1998).
- [87] Loram, J. W., Luo, J., Cooper, J. R., Liang, W. Y., Tallon, J. L., Evidence on the pseudogap and condensate from the electronic specific heat, *J. Physics and Physical Chemistry of Solids* **62**, 59-64 (2001).
- [88] Mirmelstein, A., Junod, A., Triscone, G., Wang, K.-Q., Muller, J., Specific heat of $\text{Ti}_2\text{Ba}_2\text{CuO}_6$ ("2201") 90 K superconducting ceramics in magnetic fields up to 14 T. *Physica C* **248**, 225-342 (1995).
- [89] Wen, H.-H., Mu, G., Luo, H., Yang, H., Shan, L., Ren, C., Cheng, P., Yan, J., Fan, L., Specific-heat measurement of a residual superconducting state in the normal state of underdoped $\text{Bi}_2\text{Sr}_{2-x}\text{La}_x\text{CuO}_{6+\delta}$ cuprate superconductors. *Phys. Rev. Lett.* **103**, 067002 (2009).
- [90] For the high T_c cuprates LSCO, YBCO, Ca-YBCO, BSCCO, BSLCO, TBCO, Nd-LSCO and HBCO refer to $\text{La}_{2-x}\text{Sr}_x\text{CuO}_4$ [87], $\text{YBa}_2\text{Cu}_3\text{O}_{6+x}$ [84, 87] and $\text{YBa}_2\text{Cu}_4\text{O}_8$ [91], $\text{Y}_{0.8}\text{Ca}_{0.2}\text{Ba}_2\text{Cu}_3\text{O}_{6+x}$ [56, 86], $\text{Bi}_2\text{Sr}_2\text{CaCu}_2\text{O}_{8+\delta}$ doped with 20% Pb or 15% Y [87], $\text{Bi}_2\text{Sr}_{2-x}\text{La}_x\text{CuO}_{6+\delta}$ [89], $\text{Ti}_2\text{Ba}_2\text{CuO}_{6+\delta}$ [30, 92] $\text{La}_{2-y-x}\text{Nd}_y\text{Sr}_x\text{CuO}_4$ [56], and $\text{HgBa}_2\text{CuO}_{4+\delta}$ [93], respectively.
- [91] Curro, N.J., Imai, T., Slichter, C.P., Dabrowski, B., High-temperature $^{63}\text{Cu}(2)$ nuclear quadrupole and magnetic resonance measurements of $\text{YBa}_2\text{Cu}_4\text{O}_8$. *Phys. Rev. B* **56**, 877-885 (1997).
- [92] Kubo, Y., Shimakawa, Y., Manako, T., Igarashi, H. Transport and magnetic properties of $\text{Ti}_2\text{Ba}_2\text{CuO}_{6+\delta}$ showing a δ -dependent gradual transition from an 85 K superconductor to a nonsuperconducting metal. *Phys. Rev. B* **43**, 7875-7882 (1991).
- [93] Chan, M. K., McDonald, R. D., Ramshaw, B. J., Betts, J. B., Shekhter, A., Bauer, E. D., Harrison, N. Extent of Fermi-surface reconstruction in the high-temperature superconductor $\text{HgBa}_2\text{CuO}_{4\delta}$. *Proc. Nat. Acad. Sci. USA* **117**, 9782-9786 (2020).
- [94] Curty, P., Beck, H., Thermodynamics and phase diagram of high temperature superconductors. *Phys. Rev. Lett.* **91**, 257002 (2003).
- [95] Banerjee, S., Ramakrishnan, T. V., Dasgupta, C., Phenomenological Ginzburg-Landau-like theory for superconductivity in the cuprates. *Phys. Rev. B* **83**, 024510 (2011).
- [96] Noat, Y., Mauger, A., Nohara, M., Eisaki, H., Sacks, W., How 'pairs' are revealed in the electronic specific heat of cuprates. *Solid State Commun.* **323**, 114109 (2021).
- [97] Moshe, A. G., Farber, E., Deutscher, G., Optical conductivity of granular aluminum films near the Mott metal-to-insulator transition. *Phys. Rev. B* **99**, 224503 (2019).
- [98] Pisani, L., Pieri, P., Strinati, G. C., Gap equation with pairing correlations beyond the mean-field approximation and its equivalence to a Hugenholtz-Pines condition for fermion pairs. *Phys. Rev. B* **98**, 104507 (2018).
- [99] Nakagawa, Y., Kasahara, Y., Nomoto, T., Arita, R., Nojima, T., Iwasa, Gate-controlled BCS-BEC crossover in a two-dimensional superconductor. *Science* **372**, 190-195 (2021).
- [100] In the cuprates, we have used the smaller scatter of the locations of the maxima in γ extracted from experimental data [29] (plotted in Fig. 2d) to constrain the functional form of Δ versus p in Fig. 2c by fitting. Fitting yields $T_\gamma = T_0 + T_1 p + T_2 p^2$, where $T_0 = 478 \pm 8$ K, $T_1 = -2970 \pm 110$ K and $T_2 = 4590 \pm 380$ K.
- [101] Sutherland, M., Hawthorn, D.G., Hill, R.W., Ronning, F., Wakimoto, S., Zhang, H., Proust, C., Boaknin,

- E., Lupien, C., Taillefer, L., Liang, R., Bonn, D.A., Hardy, W.N., Gagnon, R., Hussey, N.E., Kimura, T., Nohara, M., Takagi, H., Thermal conductivity across the phase diagram of cuprates: Low-energy quasiparticles and doping dependence of the superconducting gap. *Phys. Rev. B* **67**, 174520 (2003).
- [102] Mukhopadhyay, S., Sharma, R., Kim, C.K., Edkins, S.D., Hamidian, M.H., Eisaki, H., Uchida, S.-I., Kim, E.-A., Lawler, M.J., Mackenzie, A.P., Davis, J.C.S., Fujita, K., Evidence for a vestigial nematic state in the cuprate pseudogap phase. *Proc. Nat. Acad. Sci. USA* **116**, 13249-13254 (2019).
- [103] Engelbrecht, J. R., Nazarenko, A., Randeria, M., Dagotto, E., Pseudogap above T_c in a model with $d_{x^2-y^2}$ pairing. *Phys. Rev. B* **57**, 13406-13409 (1998).
- [104] van Wyk, P., Tajima, H., Hanai, R., Ohashi, Y., Specific heat and effects of pairing fluctuations in the BCS-BEC-crossover regime of an ultracold Fermi gas. *Phys. Rev. A* **93**, 013621 (2016).
- [105] Enss, T., Haussmann, R., Quantum mechanical limitations to spin diffusion in the unitary Fermi gas. *Phys. Rev. Lett.* **109**, 195303 (2012).
- [106] Tajima, H., Kashimura, T., Hanai, R., Watanabe, R., Ohashi, Y., Uniform spin susceptibility and spin-gap phenomenon in the BCS-BEC-crossover regime of an ultracold Fermi gas. *Phys. Rev. A* **89**, 033617 (2014).
- [107] Loram, J. W., Mirza, K. A., Wade, J. M., Cooper, J. R., Liang, W. Y., The electronic specific heat of cuprate superconductors. *Physica C* **235-240**, 134-137 (1994).
- [108] Alloul, H., Ohno, T., Mendels, P., ⁸⁹Y NMR evidence for a Fermi-liquid behavior in $\text{YBa}_2\text{Cu}_3\text{O}_{6+x}$. *Phys. Rev. Lett.* **63**, 1700-1703 (1989).
- [109] Johnston, D.C., Magnetic susceptibility scaling in $\text{La}_{2-x}\text{Sr}_x\text{CuO}_{4-\delta}$. *Phys. Rev. Lett.* **62**, 957-960 (1989).
- [110] Nakano, T., Oda, M., Manabe, C., Momono, N., Miura, Y., Ido, M., Magnetic properties and electronic conduction of superconducting $\text{La}_{2-x}\text{Sr}_x\text{CuO}_4$. *Phys. Rev. B* **49**, 16000-16008 (1994).
- [111] Vyaselev, O. M., Kolesnikov, N. N., Schegolev, I. F., Transition from strong to weak coupling regime with lowering T_c in $\text{Tl}_2\text{Ba}_2\text{CuO}_{6+x}$. *Physica C* **235-240**, 1613-1614 (1994).
- [112] Crocker, J., Dioguardi, A. P., apRoberts-Warren, N., Shockley, A. C., Grafe, H.-J., Xu, Z., Wen, J., Gu, G., Curro, N. J., NMR studies of pseudogap and electronic inhomogeneity in $\text{Bi}_2\text{Sr}_2\text{CaCu}_2\text{O}_{8+\delta}$. *Phys. Rev. B* **84**, 224502 (2011).
- [113] Alloul, H. in *Quantum Materials: Experiments and Theory* (Pavarini, E., Koch, E., van den Brink, J., Sawatsky, G. eds.) 13.1-13.30 (Forschungszentrum Jülich GmbH Institute for Advanced Simulation, 2016). at <<https://juser.fz-juelich.de/record/819465/files/correl16.pdf>>
- [114] In the cuprates, the T -dependences of χ_m and K are dominated by the spin susceptibility χ at a sufficiently high T compared to T_c , and in a sufficiently strong magnetic field (in the case of K), enabling χ_m and K to be considered as representative of the T -dependence of χ .
- [115] In the unitary and BEC regimes of a Fermi gas, the pseudogap at $T > T_c$ consists primarily of a gap of comparable energy to the low T pairing gap that is extensively smeared by T -dependent line broadening effects [17, 62, 83]. The line broadening is primarily associated with the loss of phase coherence above T_c . Extensive line broadening leads to a minimum in the density of states instead of a well defined gap, causing the maxima in γ and χ to become less pronounced.
- [116] Chen, Q. J. *Generalization of BCS theory to short coherence length superconductors: A BCS-Bose-Einstein crossover scenario*. Ph.D. thesis, University of Chicago (2000). (freely accessible in the ProQuest Dissertations & Theses Database online).
- [117] Chen, Q., Levin, K., Kosztin, I., Superconducting phase coherence in the presence of a pseudogap: Relation to specific heat, tunneling, and vortex core spectroscopies. *Phys. Rev. B* **63**, 184519 (2001).
- [118] Cooper, J. R., Loram, J. W., The normal state gap and other strange properties of cuprate superconductors. *J. Phys. IV France* **10**, Pr3-213-224 (2000).
- [119] Božović, I., He, X., Wu, J., Bollinger, A. T., Dependence of the critical temperature in overdoped copper oxides on superfluid density. *Nature* **536**, 309-311 (2016).
- [120] Although it may also be affected by its co-location with stripe-ordering in this system; Ma, Q., Rule, K. C., Cronkwright, Z. W., Dragomir, M., Mitchell, G., Smith, E. M., Chi, S., Kolesnikov, A. I., Stone, M. B., Gaulin, B. D., Parallel spin stripes and their coexistence with superconducting ground states at optimal and high doping in $\text{La}_{1.6-x}\text{Nd}_{0.4}\text{Sr}_x\text{CuO}_4$. *Phys. Rev. Research* **3**, 023151 (2021).
- [121] Cooper, R. A., Wang, Y., Vignolle, B., Lipscombe, O. J., Hayden, S. M., Tanabe, Y., Adachi, T., Koike, Y., Nohara, M., Takagi, H., Proust, C., Hussey, N. E. Anomalous criticality in the electrical resistivity of $\text{La}_{2-x}\text{Sr}_x\text{CuO}_4$. *Science* **323**, 603 (2009).
- [122] Giraldo-Gallo, P., Galvis, J. A., Stegen, Z., Modic, K. A., Balakirev, F. F., Betts, J. B., Lian, X., Moir, C., Riggs, S. C., Wu, J., Bollinger, A. T., He, X., Božović, I., Ramshaw, B. J., McDonald, R. D., Boebinger, G. S., Shekhter, A., Scale-invariant magnetoresistance in a cuprate superconductor. *Science* **361**, 479-481 (2018).
- [123] Legros, A., Benhabib, S., Tabis, W., Laliberté, F., Dion, M., Lizaïre, M., Vignolle, B., Vignolles, D., Raffy, H., Li, Z. Z., Auban-Senzier, P., Doiron-Leyraud, N., Fournier, P., Colso, D., Taillefer, L., Proust, C., Universal T -linear resistivity and Planckian dissipation in overdoped cuprates. *Nature Phys.* **15**, 142-147 (2019).
- [124] Zaanen, J., Planckian dissipation, minimal viscosity and the transport in cuprate strange metals. *SciPost Phys.* **6**, 061 (2019).
- [125] Cao, C., Elliott, E., Joseph, J., Wu, H., Petricka, J., Schafer, T., Thomas, J. E., Universal quantum viscosity in a unitary Fermi gas, *Science* **331**, 58-61 (2010).
- [126] Enss, T., Quantum critical transport in the unitary Fermi gas. *Phys. Rev. A* **86**, 013616 (2012).
- [127] Pistolesi, F., Strinati, G. C., Evolution from BCS superconductivity to Bose condensation: Calculation of the zero-temperature phase coherence length. *Phys. Rev. B* **53**, 15168-15192 (1996).
- [128] Engelbrecht, J. R., Randeria, M., Sá de Melo, C. A. R., BCS to Bose crossover: Broken-symmetry state. *Phys. Rev. B* **55**, 15153-15156 (1997).
- [129] Grissonnanche, G., Cyr-Choinière, O., Laliberté, F., René de Cotret, S., Juneau-Fecteau, A., Dufour-Beauséjour, S., Delage, M.-È., LeBoeuf, D., Chang, J., Ramshaw, B. J., Bonn, D. A., Hardy, W. N., Liang, R., Adachi, S., Hussey, N. E., Vignolle, B., Proust,

C., Sutherland, M., Krämer, S., Park, J.-H., Graf, D., Doiron-Leyraud, N., Taillefer, L. Direct measurement of the upper critical field in cuprate superconductors. *Nature Commun.* **5**, 3280 (2014).

SUPPLEMENTARY INFORMATION

Introduction

This Supplementary Information document contains the following: data pertaining to $\delta\gamma(T_c)$ in conventional BCS superconductors and Fe- and Ni-based superconductors; information about cuprate hole dopings p used in constructing graphs in the main paper; raw γ and χ data including the locations of T_γ and T_χ used in the main paper; Knight shift data on BLSCO; a discussion pertaining to prior modeling of $\delta\gamma(T_c)$ versus p by Chen *et al.*; details concerning cold atomic gas data used in the main paper; estimates of the gap ratio at the unitary point of a cold atomic gas; a discussion of the thermodynamics of maxima in γ and χ ; coherence length estimates in various cuprates based on H_{c2} or the upper extent in magnetic field for the vortex solid phase; estimates of the Fermi energy in the cuprates; a discussion of the higher values of p^* in cuprates with lower T_c 's; the origin of the 'Fermi arcs;' the T -dependence of the antinodal gap; lifetime effects on N_0 in a cold atomic Fermi gas; the choice of a smaller gap option for Δ in the cuprates; evidence for a hidden maximum in the normal state heat capacity data of a cold atomic Fermi gas; and reports of peaks in $\delta\gamma(T_c)$, γ and m^* associated with quantum criticality.

$\delta\gamma(T_c)/\bar{\gamma}$ for conventional BCS and Fe- and Ni-based superconductors.

Figure 4a shows $\delta\gamma(T_c)/\bar{\gamma}$ (where $\bar{\gamma}$ is an assumed constant normal state Sommerfeld coefficient) of various conventional BCS superconductors as a function of $2\Delta/k_B T_c$ from Ref. [78]. The outliers with lower values of $\delta\gamma(T_c)/\bar{\gamma}$ correspond to amorphous materials. Apart from the outliers, $\delta\gamma(T_c)/\bar{\gamma}$ can be seen to steadily increase with $2\Delta/k_B T_c$, but never reaching the magic gap ratio value of ≈ 6.5 .

Figure 4b shows $\delta\gamma(T_c)/\bar{\gamma}$ versus $2\Delta/k_B T_c$ for various Fe- and Ni-based superconductors, using data from Ref. [79]. Here, the system with the largest $\delta\gamma(T_c)/\bar{\gamma}$ value has a gap ratio $2\Delta/k_B T_c = 6.6$, which is therefore consistent with an optimally robust superconducting state.

A caveat with renormalization by $\bar{\gamma}$ is that this quantity is unlikely to be accurately determined by experiment once $2\Delta/k_B T_c \gtrsim 6.5$, due to the formation of a pseudogap, which causes γ to be a non monotonic function of T .

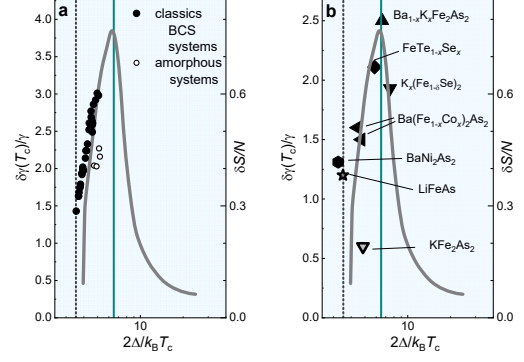


FIG. 4. $\delta\gamma(T_c)$ data in other superconductors. **a**, $\delta\gamma(T_c)/\bar{\gamma}$ values for conventional BCS superconductors from Ref. [78]. Open symbols represent amorphous superconductors for which $\delta\gamma(T_c)/\bar{\gamma}$ is reduced. **b**, $\delta\gamma(T_c)/\bar{\gamma}$ values for various Fe- and Ni-based superconductors from Ref. [79]. The grey lines correspond to δS for a cold atomic Fermi gas, as plotted in the main paper.

In the cuprates, owing to a significant deviation of γ from a constant value at $T > T_c$, due primarily to the pseudogap, we plot the absolute value of $\delta\gamma(T_c)$ rather than the ratio $\delta\gamma(T_c)/\bar{\gamma}$. This avoids incurring errors associated with estimating a constant $\bar{\gamma}$, as is typically done in BCS superconductors. We plot only the absolute value of $\delta\gamma(T_c)$ also for the case of a cold atomic gas, where this may also be the case.

Cuprate hole dopings

For LSCO, the hole dopings p are determined using $p = x$ [87]. For YBCO, in the case of $\text{YBa}_2\text{Cu}_3\text{O}_{6+x}$ they are determined from the value of T_c using Ref.[32], in the case of Ca-YBCO (YBCO in which 20% of the Y is substituted with Ca), we have used p values from Ref.[56], while in the case of $\text{YBa}_2\text{Cu}_4\text{O}_8$ (data for $p = 0.125$) we have used p from Ref.[33]. For BSCCO, p values are provided in Ref.[87], for BSLCO p is provided in Ref.[89], while for TBCO, p is obtained by applying the Tallon formula[34] to the data in Ref.[85], while it is assumed that $p = 0.16$ in Ref.[88]. For YBCO in Figs. 2 and 3 of the main paper, the highest two compositions ($p = 0.152$ and 0.158) are for samples in which 2% of the planar Cu has been substituted with Zn.

For LSCO and Nd-LSCO, additional T_c values in Fig. 1c of the main paper are obtained from Refs. [31, 120].

For TBCO, γ data pertains to a sample in which T_c is suppressed by a magnetic field[30]. Although it remains unclear to what extent the field suppresses the phase stiff-

ness of the superconducting state relative to the pairing gap, the maximum in γ presented at $B = 13$ T pertains to the resistive regime[45] (the zero resistance state being almost completely suppressed). There is also relatively little change in the maximum between 10 and 13 T. Measurements on a non superconducting composition nearby in doping have enabled the phonon contribution to the heat capacity to be subtracted with reasonable accuracy[30].

Determination of T_γ and T_χ from the original cuprate data.

Figure 5 shows the data from Fig. 1 of the main paper[30, 84, 87, 91, 92, 108–110, 113], here plotted as a function of the actual temperature T . T_γ and T_χ are obtained from the location of the maxima in T . In the case of noisier datasets, or datasets with fewer points, the location of the maxima is assisted by the fitting of a third order polynomial in $\ln T$. We make an exception for the $p = 0.22$ composition of LSCO, where we read off the temperature at which T_χ exhibits a shoulder feature. The temperatures (T_γ and T_χ), at which maxima are observed, are plotted in Fig. 2d of the main paper. Owing to the broad widths of the maxima, the error bars are 10% and 20% for T_γ and T_χ , respectively.

By using published temperature-dependent γ and χ data, we rely on background subtractions made by the authors of the respective works. For γ , systematic errors are likely to be introduced owing to the complicated phonon spectra and the reliance on non-superconducting reference samples. Owing to assumptions that need to be made to account for changes in the concentration of O doped into the CuO chains that are necessary to produce changes in hole doping[84], these systematic errors become largest at higher dopings of YBCO. Meingast *et al.* have shown that it is challenging to accurately model the phonon modes in this system using *AB-initio* methods[35]. However, at the same O dopings where systematic errors in accounting for the phonon contribution are expected to become most significant, a peak in γ is no longer visible owing to its concealment by superconductivity. The jump $\delta\gamma(T_c)$ in γ at T_c , by contrast, is unaffected by the phonon subtraction.

In the case of χ , measurements of K are made in the presence of a uniform magnetic field for which the effect of incipient diamagnetism above T_c is greatly reduced relative to measurements of the uniform susceptibility. The temperature dependence of K is therefore primarily attributed to changes in the spin susceptibility. Incipient diamagnetism, mostly in the overdoped cuprates, can in some cases produce a maximum in χ that is unrelated to pair amplitude fluctuations or the pseudogap. Owing to its lower T_c values, measurements of the uniform susceptibility are less prone to the effects of incipient dia-

magnetism in LSCO. There is evidence for a diamagnetic contribution to χ_m of BSCCO and TBCO at the lowest temperatures[87, 92], which we have cutoff in cases where this contribution becomes obtrusively large.

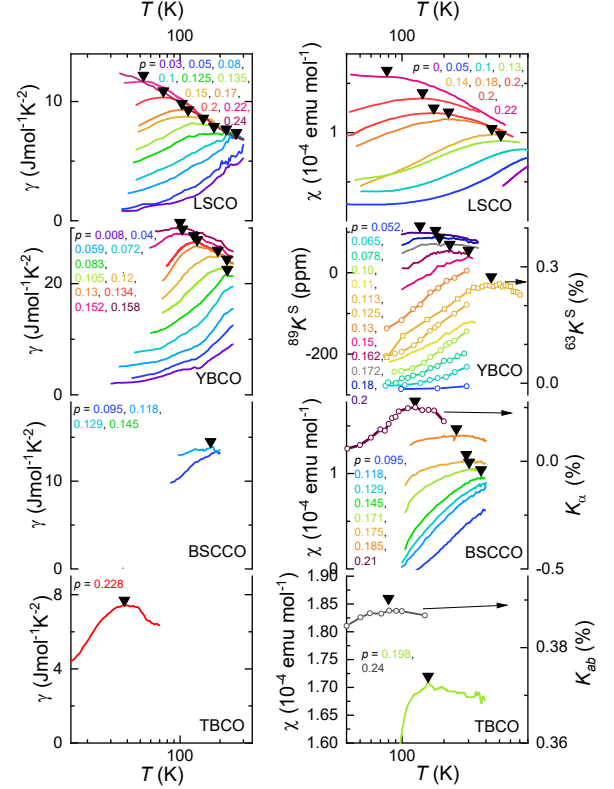


FIG. 5. **Raw data.** Data used in Fig. 3 of the main paper plotted as a function of the actual temperature T . The inferred maximum are indicated by inverted triangles.

BSLCO Knight shift data

Knight shift data also exists for BSLCO (or $\text{Bi}_2\text{Sr}_{2-x}\text{La}_x\text{CuO}_{6+\delta}$), in which a downturn has previously been reported to occur at temperatures below T^* [36] (see Fig. 6). This downturn is most clearly apparent on plotting the data versus $2\Delta/k_B T$. While K in BSLCO supports the existence of a maximum at $2\Delta/k_B T \approx 3$, it was not measured to sufficiently high temperature in this experiment to determine this unambiguously. One possible exception is the sample with a hole doping of $p \approx 0.206$.

Prior modeling of $\delta\gamma(T_c)$ versus p

One strong coupling theory of superconductivity that has been shown to qualitatively account for the strong variation of $\delta\gamma(T_c)$ with p [116, 117]. In this model, the

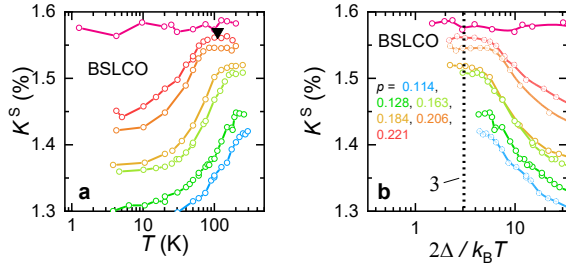


FIG. 6. **Raw data in BSLCO.** **a**, Knight shift in BSLCO. **b**, Knight shift in BSLCO plotted versus $2\Delta/k_B T$, using doping values from Ref. [36].

total jump in $\delta\gamma(T_c)$ is the sum of a vertical jump resulting from the onset of a superconducting order parameter Δ_s and a lambda anomaly-like increase immediately above T_c resulting from line broadening effects relating to the pseudogap Δ_{pg} on approaching T_c . The two are assumed to add in quadrature: i.e. $\Delta = \sqrt{\Delta_s^2 + \Delta_{pg}^2}$. In order to produce a variation in $\delta\gamma(T_c)$ with p similar to that in experiments, it was necessary to assume an arbitrary functional form of the line broadening γ_l near T_c of the pseudogap on T and on the overall magnitude of Δ_{pg} as a function of p in this theory. This is in contrast to the modeling of Haussmann *et al.*[14], for which we find consistency with $\delta\gamma(T_c)$ in the cuprates despite no attempt having been made to adjust the parameters of the theory to fit cuprate data.

Cold atomic Fermi gas data

In Fig. 1 of the main paper, T_c , $\delta\gamma(T_c)$, δS and Δ are extracted from Figs. 4, 5, 6 and 8 of Haussmann *et al.*[14]. The multivaluedness of $S(T)$ in the vicinity of T_c is known to be an artifact of the numerical method. We make two estimates of $\delta\gamma(T_c)$ in order to obtain a lower and upper bound.

In order to obtain a lower bound estimate for $\delta\gamma(T_c)$ (in Fig. 1b of the main paper) from Ref. [14], $S(T)$ is differentiated with respect to T in the superfluid state, where the functional form is exponential in temperature, and in the normal state, where it is monotonically varying with T . $\delta\gamma(T_c)$ is then taken as the difference in $\partial S/\partial T$ between the superfluid and normal states at T_c (see Fig. 7). The main limitation of this lower bound approximation is that that does not fully account for entropy of the normal state for $1/k_F a \geq 0$. The problem is that $S(T)$ within the superfluid phase rises very steeply on the approach to T_c , deviating from exponential behavior, very close to

the transition.

For an upper bound estimate of $\delta\gamma(T_c)$ (in Fig. 1b of the main paper), we use the approximation $\delta\gamma(T_c) \approx \frac{\delta S}{\delta T} - \frac{\partial S_n}{\partial T}$, where δT is the interval in T over which S is multivalued, δS is the full extent of the variation in S within the interval and $\frac{\partial S_n}{\partial T}$ is the slope of S in the normal state.

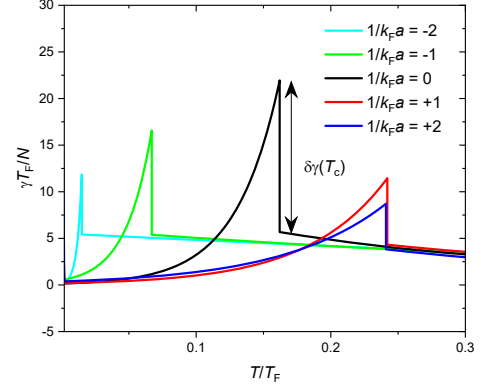


FIG. 7. **Phase transition anomaly in the unitary regime of a Fermi gas.** γ is extracted from $S(T)$ in Ref. [14] as described in the text.

In Fig. 3 of the main paper, γ is obtained by differentiating S in Fig. 19 of Chen and Wang[62]. Owing to the intersection of T_γ and T_c at $1/k_F a = 0$, tuning of $1/k_F a$ into the BEC regime is required in order to observe the maxima in γ [62].

Estimates of $2\Delta/k_B T_c$ at the unitary point of a cold atomic gas

From the various theoretical methods tabulated in Table 1 of Ref. [16] and obtained from Ref. [97], we obtain $2\Delta/k_B T_c = 6.6 \pm 0.1$. The experimental estimate of the gap ratio at the unitary point is $2\Delta/k_B T_c = 5.3 \pm 0.8$ [16], on combining quoted experimental errors in Δ and T_c . Combining experimental and numerical estimates, we obtain $2\Delta/k_B T_c = 6.5 \pm 0.2$.

Thermodynamics of the maxima in γ and χ .

Gap in an electronic band.

For a gap opening in an electronic band obeying Fermi-Dirac statistics, we consider the electronic contribution to the Helmholtz free energy

$$F_{\text{el}} = -N_A \sum_{\sigma=\pm s} \int_{-\infty}^{\infty} k_B T D(\varepsilon + sg\mu_B B) \ln(1 + e^{-\frac{\varepsilon - \mu}{k_B T}}) d\varepsilon + N_A N \mu,$$

as an integral over states, where

$$D(\varepsilon + sg\mu_B B)$$

is the density of states subject to Zeeman splitting $sg\mu_B B$ (where s is the spin, g is the g -factor and μ_B is the Bohr magneton). If we consider the energy of a single electronic band subject to Zeeman splitting, then spin singlet gap formation couples electron and hole states of like

spin (or electrons or holes of opposite spin) whereas spin triplet formation couples electrons and holes of opposite spin.

Under the assumption of a symmetric gap centered on the chemical potential (defined as $\mu = 0$) and a constant number of particles N , the electronic coefficient of the heat capacity and the spin susceptibility are given by[37, 38]

$$\gamma = \frac{C_{\text{el}}}{T} = \left. \frac{\partial^2 F_{\text{el}}}{\partial T^2} \right|_{V,N} = N_A \int_{-\infty}^{\infty} D(\varepsilon) \frac{\varepsilon^2}{k_B T^3} \frac{e^{\varepsilon/k_B T}}{(e^{\varepsilon/k_B T} + 1)^2} d\varepsilon \quad (1)$$

and

$$\chi = \mu_0 \left. \frac{\partial^2 F_{\text{el}}}{\partial B^2} \right|_{V,N} = \mu_0 (sg\mu_B)^2 N_A \int_{-\infty}^{\infty} D(\varepsilon) \frac{1}{k_B T} \frac{e^{\varepsilon/k_B T}}{(e^{\varepsilon/k_B T} + 1)^2} d\varepsilon, \quad (2)$$

respectively, in the limit $B \rightarrow 0$ where $s = \frac{1}{2}$.

Trivial gap in a narrow electronic band ($t \rightarrow 0$)

When a gap 2Δ opens in a narrow electronic band, the resulting trivially gapped state consists of two narrow levels centered about μ . One can model the density of states resulting from spin singlet bound state formation as delta functions so that $D(\varepsilon) = \delta(|\varepsilon \pm sg\mu_B B| - \Delta)$, for which we obtain

$$\gamma = 2N_A \frac{\Delta^2}{k_B T^3} \frac{e^{\Delta/k_B T}}{(e^{\Delta/k_B T} + 1)^2} \quad (3)$$

and

$$\chi = \mu_0 (sg\mu_B)^2 N_A \frac{1}{k_B T} \frac{e^{\Delta/k_B T}}{(e^{\Delta/k_B T} + 1)^2}, \quad (4)$$

respectively. We locate the maxima in γ and χ by setting $\partial\gamma/\partial T = 0$ and $\partial\chi/\partial T = 0$, yielding the transcendental equations $3\theta_\gamma^{\text{max}} = \tanh(1/2\theta_\gamma^{\text{max}})$ and $\theta_\chi^{\text{max}} = \tanh(1/2\theta_\chi^{\text{max}})$, for which we obtain $\theta_\gamma^{\text{max}} = k_B T_\gamma/\Delta \approx 0.308296$ and $\theta_\chi^{\text{max}} = k_B T_\chi/\Delta \approx 0.647918$; hence $2\Delta/k_B T_\gamma \approx 6.4873$ and $2\Delta/k_B T_\chi \approx 3.0868$.

For spin triplet bound state formation, the density of states has the form $D(\varepsilon) = \delta(|\varepsilon| - \sqrt{\Delta^2 + (sg\mu_B B)^2})$, yielding the same γ as given by Equation (3). However, for a spin triplet bound state, $\chi = 0$ in the limit $B \rightarrow 0$.

d-wave and s-wave electronic gaps in a simple tight binding dispersion

For the d -wave gap used to model the peaks in γ and χ in Fig. 3 of the main paper, the electronic density of states is given by $D(\varepsilon) = \frac{1}{\pi^2} \frac{\partial}{\partial \varepsilon} \int_0^\pi k_y(\varepsilon) dk_x$, where we consider a conventional two-dimensional tight-binding dispersion

$$\varepsilon = \sqrt{4t^2(\cos k_x + \cos k_y)^2 + \frac{\Delta^2}{4}(\cos k_x - \cos k_y)^2}$$

with a conventional d -wave gap and an assumed in-plane hopping $5t = 3\Delta$. For simplicity we neglect higher order hopping terms and set $p = 0$ (i.e. half filling). In this case the integrals for γ and χ are performed numerically, and we obtain $\theta_\gamma^{\text{max}} = k_B T_\gamma/\Delta \approx 0.311$ and $\theta_\chi^{\text{max}} = k_B T_\chi/\Delta \approx 0.683$; hence $2\Delta/k_B T_\gamma \approx 6.43$ and $2\Delta/k_B T_\chi \approx 2.93$. In the case of an s -wave gap, we simply use

$$\varepsilon = \sqrt{4t^2(\cos k_x + \cos k_y)^2 + \Delta^2}.$$

Coherence length

Figure 8a shows the coherence length ξ_0 estimated for a cold atomic Fermi gas[128] while Fig. 8b shows the in-plane coherence length estimated from H_{c2} using

$H_{c2} = \Phi_0/2\pi\xi_0^2$, where H_{c2} is itself estimated by extrapolating fits of the vortex melting line as a function of temperature [39, 93, 129].

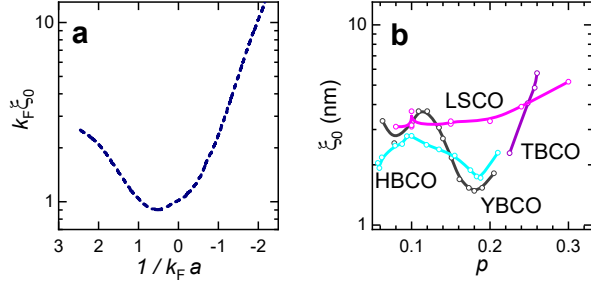


FIG. 8. **Coherence lengths.** **a**, Coherence length ξ_0 versus $1/k_F a$ for a cold atomic Fermi gas [39, 93, 129]. **b**, Estimates of the in-plane coherence length as a function of p in various cuprates.

The Fermi energy in the cuprates

One way to infer proximity to a BCS-BEC crossover is to determine the ratio $k_B T_c / \varepsilon_F$, where $T_F = k_F \varepsilon_F$ is the Fermi temperature. At the unitary point, experimental and Quantum Monte Carlo studies have shown that in a three-dimensional system, this ratio reaches a maximum value of $k_B T_c / \varepsilon_F \approx 0.17$ whereas in a ideal two-dimensional system it reaches a maximum value of $k_B T_c / \varepsilon_F \approx 0.125$ [18]. Both of these estimates assume a parabolic band approximation. In the BCS and BEC regimes, $k_B T_c / \varepsilon_F$ falls below this value, with the reduction being most severe in the BCS limit.

Assuming a parabolic band approximation, magnetic quantum oscillations measurements of the frequency F and effective mass m^* provide an estimate of the Fermi energy via the ratio $\varepsilon_F = \hbar e F / m^*$. In the overdoped regime, quantum oscillation measurements pertain to the entire Fermi surface. Using average values $F = 17.8$ kT and $m^* = 5.2 m_e$ (where m_e is the free electron mass) in TBCO [40], we obtain $\varepsilon_F \approx 400$ meV. From this we obtain $k_B T_c / \varepsilon_F \approx 0.006$ (using $T_c = 26$ K for the highest transition temperature of samples exhibiting quantum oscillations). This ratio is consistent with the very overdoped cuprate TBCO being deep in the BCS regime.

Recent studies of the low temperature Sommerfeld coefficient of Eu- and Nd-substituted LSCO [56] have suggested that the effective mass could increase by as much as a factor of 4 with decreasing hole doping, reaching a maximum value around $p = 0.23$ in that specific material. If a similar 4-fold increase in m^* occurs in TBCO, then this combined with its higher maximum $T_c \approx 96$ K would produce a somewhat larger estimate of the ratio $k_B T_c / \varepsilon_F \approx 0.09$ — a value much closer to that expected in the unitary regime. Realization of the unitary regime

is therefore plausible from the perspective of quantum oscillation and heat capacity measurements.

In the underdoped regime of YBCO, quantum oscillation studies have found much smaller sections of Fermi surface with the effective mass exhibiting a non-monotonic behavior as a function of p [55]. Close to optimal T_c at $p = 0.153$ (where $T_c \approx 92$ K and $F \approx 600$ T), $m^* \approx 3.6 m_e$. This then falls to $m^* \approx 1.4 m_e$ at $p = 0.116$ (where $T_c \approx 67$ K and $F \approx 560$ T) before increasing again to $m^* \approx 4.6 m_e$ at $p = 0.09$ (where $T_c \approx 57$ K and $F \approx 510$ T). This yields Fermi energies in the range $13 \leq \varepsilon_F \leq 46$ meV and $0.3 \leq k_B T_c / \varepsilon_F \leq 0.6$. These values of $k_B T_c / \varepsilon_F$ significantly exceed that expected at the unitary point. Based on Hall effect and other measurements [41], however, these small pockets are the product of a broken symmetry phase that reconstructs the Fermi surface.

In a BEC scenario, we might expect the pairing to onset at temperatures significantly higher than the onset of Fermi surface reconstruction. Provided the orbitally-averaged Fermi velocity v_F of the quasiparticles on the small pocket is similar to that of the quasiparticles on the the unreconstructed Fermi surface (which is generally true for translational symmetry breaking) and the parabolic approximation remains valid, we might expect the unreconstructed Fermi energy to be given by $\varepsilon_F = \hbar^2 k_F^2 / 2 = (\hbar/2) v_F k_F$, where k_F is the orbitally-averaged Fermi radius. We might therefore expect ε_F to scale as $\varepsilon_F \propto k_F \propto \sqrt{F}$, where $F \propto (1+p)$ for an unreconstructed Fermi surface consistent with Luttinger's theorem. Assuming such scaling, we obtain unreconstructed Fermi energies in the range $80 \lesssim \varepsilon_F \lesssim 270$ meV, yielding $0.02 \lesssim k_B T_c / \varepsilon_F \lesssim 0.07$. The upper limit of this $k_B T_c / \varepsilon_F$ estimate is a significant fraction of that ($k_B T_c / \varepsilon_F \approx 0.125$) expected at the unitary point in a two-dimensional system, which is therefore consistent with the pairing having crossed over into the BEC regime in underdoped YBCO.

Differences in p^* between cuprates with high and low T_c 's

Figure 1c of the main paper reveals what appear to be significant differences between cuprates that attain high values of $T_c \sim 100$ K and those that do not. From the requirement that T_γ and T_c intersect in order for superconductivity to become optimally robust, we can now understand why $\delta\gamma(T_c)$ is peaked at different values of p^* in different cuprate families, and not at all in others (e.g. BSLCO) [56, 84–89]. In the case of YBCO, Ca-YBCO, BSCCO and TBCO, the observation of pronounced peaks in $\delta\gamma(T_c)$ at p^* strongly suggests that these systems undergo a BEC to BCS crossover as a function of p . In the case of LSCO, by contrast, T_c appears not to reach a sufficiently high value for it to intersect with T_γ until sig-

nificantly higher dopings, giving rise to a much broader peak in $\delta\gamma(T_c)$. By extrapolation, we estimate $p \approx 0.26$ for LSCO in Fig. 1c of the main paper, suggesting that it has a increased inclination to remain within the BEC regime over a wider range of p , as has also recently been concluded from measurements of the superfluid density as a function of p [119]. BSLCO and Nd-LSCO appear to lie even deeper in the BEC regime (see Fig. 1a and b of the main paper), on account of their small T_c and tiny $\delta\gamma(T_c)$ values. Factors that could contribute (by way of a reduced superfluid density [22]) in LSCO, BSLCO and Nd-LSCO to an increased tendency for these systems to remain in the BEC limit include their closer proximities to a van Hove singularity in the electronic structure [?] and increased levels of disorder [42]. For example, systematic studies of disorder have shown this to suppress T_c and the superfluid density in a proportionate manner at low p , giving rise to a superconductor-to-insulator transition [43, 44].

‘Fermi arcs’

It is debated whether these arcs are intrinsic to a normal state d -wave pairing gap [103], are the consequence of phase fluctuations primarily affecting the d -wave nodes [46, 47], or are the product of a co-existing charge-density wave [60, 61] or a pair-density wave [48, 49] phase.

T -dependence of the antinodal gap

Spectroscopic measurements (including measurements made on the same composition [50, 51]) differ on the degree to which the antinodal gap decreases with increasing temperature. Our finding of a quantitative consistency between Figs. 2c and d of the main paper supports a scenario in which the antinodal gap is largely unsuppressed at $T = T_\gamma$.

Lifetime effects on N_0 in cold atomic Fermi gas measurements

For N_0 , we assume the experimentally quoted conversion between the tuning magnetic field and $1/k_F a$ [12, 13]. Measurements of N_0 are affected by lifetime effects. Since the lifetime is also longest at the unitary point, corresponding to $1/k_F a = 0$, this can cause the measured peak in N_0 to become sharper than that in $\delta\gamma(T_c)$. In Ref. [12], the experimental uncertainty in the location of the unitary point in $1/k_F a$ is ≈ 0.2 while in Ref. [13] it is ≈ 0.03 . The lower uncertainty of the latter may account for its greater similarity to $\delta\gamma(T_c)$.

Alternative choice of a smaller gap for Δ in the cuprates

An alternative option is that Δ corresponds to a smaller secondary gap [71] comparable in energy to the $\mathbf{q} = (\pi, \pi)$ resonance energy seen in neutron scattering measurements. Apart from having a much weaker spectral weight and also having no reported signature in γ or χ , this gap yields a near constant gap ratio: $2\Delta/k_B T_c \approx 5$ [71], placing it within the BCS regime that is usually adequately accounted for by Eliashberg theory in other superconductors [78]. Such a constant gap ratio would, however, cause all of the $\delta\gamma(T_c)$ data points to be stacked vertically at a constant $2\Delta/k_B T_c$ in Fig. 2a of the main paper. Such behavior is in contravention of the strong dependence of $\delta\gamma(T_c)$ on $2\Delta/k_B T_c$ in known boson-mediated (i.e. BCS) superconductors [78].

Evidence for a hidden maximum in the heat capacity of a cold atomic gas

In the case of heat capacity measurements on a cold atomic Fermi gas [11], a pseudogap with the same energy as the pairing gap Δ is expected to produce a maximum in C at $T/T_F \approx 0.176$. A maximum at this location cannot be observed owing to its proximity to T_c at the unitary point. The $\approx 40\%$ deviation of the normal state C from that of a non interacting Fermi gas in the region of the normal state just above T_c is, however, consistent with a pseudogap [11]. The normal state γ (in the absence of a superfluid transition) would need to exhibit a downturn at low temperatures in order to conserve entropy.

Peaks in $\delta\gamma(T_c)$, γ and m^* associated with quantum criticality

The peak in $\delta\gamma(T_c)$ as a function of p for Ca-YBCO in Fig. 1c of the main paper was recently attributed to a $T = 0$ maximum in the normal state effective mass or γ at p^* [56]. However, in Fig. 3a of the main paper we find it to coincide with a finite temperature maximum in γ originating from excitations across Δ . Hence, the maximum in γ coincides with p^* only at $T = T_c$.

Given the thermodynamic evidence for the continued presence of a normal state gap at $p > p^*$ in Fig. 2d of the main paper, the peak in $\delta\gamma(T_c)$ at $T_c = T_\gamma$ could not be easily understood were the normal state gap to have a non pairing origin [52]. For a non pairing gap, we would expect the peak in $\delta\gamma(T_c)$ to occur only as the normal state gap vanishes, as has been found experimentally at the antiferromagnetic quantum phase transition in heavy fermion superconductors [53] and in thermodynamic simulations of a non-pairing pseudogap state crit-

ical point [54, 75].

The reported peaks in m^* and γ at low T are at tem-

peratures $T \lesssim 10$ K [55, 56], implying that their contributions to S_n near T_c are overwhelmed by much larger contributions from excitations across Δ .